IOP Conf. Series: Materials Science and Engineering **1345** (2026) 012006 doi:10.1088/1757-899X/1345/1/012006

Assessing the Adhesion of Nanofibrous PVDF-HFP as Passive Thermal Control Coatings for the Extraterrestrial Storage of Cryogenic Propellants

Chieloka Ibekwe[1], Adrien Neveu[1], Nan An[1], Xuanjie Wang[1], Jason Hartwig[2], Adam Swanger[3] and Shankar Narayan[1*]

[1] Department of Mechanical, Aerospace and Nuclear Engineering, Rensselaer Polytechnic Institute, Troy, NY 12180, USA
[2] NASA Glenn Research Center, Cleveland, OH 44135, USA
[3] NASA Kennedy Space Center, Cryogenics Test Laboratory, FL 32899, USA

[*]E-mail: narays5@rpi.edu

Abstract. Cryogenic propellant passive thermal management techniques in space are essential complements to active thermal management methods, helping reduce absolute dependence on the latter. Particularly, materials with superior optical properties (high solar reflectance and infrared emittance) would be beneficial for passive thermal control to reject most of the incident solar radiation and enhance thermal emission from the storage tank, leading to self-cooling. We developed a nanofibrous, porous passive thermal control material by electrospinning polyvinylidene fluoride-co-hexafluoropropylene (PVDF-HFP) co-polymer onto an aluminum foil substrate. The material exhibits a very high solar reflectance (>99%) and infrared emittance (~86%) when characterized in the ultraviolet-visible-near infrared and mid-infrared wavelengths. This study focuses on the adhesion of the nanofibrous PVDF-HFP to the substrate. We incorporated in-lab fabricated and commercial adhesives, under normal room conditions, between the nanofibers and the aluminum foil substrate to improve their adhesion. Some samples were also exposed to space-like conditions – vacuum and thermal cycling, to investigate their effects on the strengths of adhesives. Subsequently, adhesion peel tests were conducted on all the samples to assess the peel strengths of the bonds. Peel test strengths after space environment conditioning of the adhesives were generally higher than those observed in the pristine, unaged samples. The results are discussed in this study.

1. Introduction

Future space missions to distant frontiers could require significantly larger amounts of cryogenic propellants than typical missions. Such missions and esoteric applications, like space tourism, would benefit from propellant storage in space for refueling space vehicles. In this regard, advancements in cryogenic fluid management are necessary to achieve extraterrestrial storage. Specifically, passive cryogen management techniques in space, like radiative cooling, are necessary to reduce the burden on active thermal control methods, like cryocoolers. Materials with superior optical properties (high solar reflectance and infrared emittance) [1–3] would find useful passive thermal control applications by rejecting most of the incident solar radiation, facilitating thermal emission from the storage tank (enabling self-cooling), and managing inward heat loads [4,5]. In this study, we manufactured a passive thermal control material by electrospinning [6,7] polyvinylidene fluoride-co-hexafluoropropylene

(PVDF-HFP) co-polymer onto an aluminum foil substrate. The electrospun PVDF-HFP has a porous structure consisting of nanofibers as observed by scanning electron microscopy. Spectrophotometric characterization of the optical properties in the ultraviolet-visible-near infrared and mid-infrared wavelengths reveal that the material exhibits a very high solar reflectance (>99%) and infrared emittance (86%), which are necessary for effective radiative thermal management.

Despite the excellent optical properties and thermal insulation performance of the nanofibers, they are prone to delamination from a smooth, non-porous substrate**.** The nanofibrous materials are usually electrospun on a substrate to provide better mechanical support and delamination from the substrate could occur because the nanoscale interfacial contact regions between each individual fiber and substrate may not be sufficient for complete mechanical interlocking [8] needed for the formation of strong bonds. Furthermore, residual electrical charges which build up on the nanofibrous coatings when electrospinning thicker coatings and are not completely dissipated to the ground could lead to interlayer delamination along the thickness of the nanofibrous network. [9]

Therefore, it is necessary to improve the adhesion between the layers of the nanofibrous network, as well as the adhesion to the substrate. PVDF-HFP nanofibers manufactured in this study are not prone to nanofibrous interlayer debonding, hence we focused on studying and improving their adhesion to the aluminum foil substrate. One common way to improve nanofiber-substrate adhesion is by applying adhesives [10], and we employed this method in this study. We applied commercial adhesives, as well as an in-lab fabricated adhesive (styrene-ethylene-butylene-styrene thermoplastic elastomer) between the adherends and characterized the bond strengths by conducting peeling tests, at normal room conditions, using an Instron universal testing machine. To simulate extraterrestrial conditions that subject the materials to vacuum and extreme temperature swings, we exposed some of the samples under investigation to vacuum and thermal cycling between cryogenic and high temperatures. Subsequently, the adhesive peel strengths were characterized and compared with normal conditions and the results are discussed in this paper.

2. Methodology

2.1 Materials and Solution Preparation

Polyvinylidene fluoride-co-hexafluoropropylene (average M_w ~400,000, average M_n ~130,000) in pellet form was obtained from Sigma-Aldrich. N,N-Dimethylformamide (DMF) solvent was purchased from Spectrum Chemical, and acetone (99.5 %) was obtained from VWR Chemicals BDH. Styrene-Ethylene-Butylene-Styrene (SEBS), a linear triblock copolymer of styrene and ethylene/butylene was obtained as a powder from Kraton™ (G1652M). Chloroform and xylene were purchased from Macron Fine Chemicals, and toluene was purchased from Thermo Scientific Chemicals. Commercial-off-the-shelf adhesives like Loctite® Power Grab® Ultimate Crystal Clear and Permatex® Silicone RTV 80050 Clear Adhesive Sealant were purchased and used for comparison of adhesive resistance-to-peel strengths.

The PVDF-HFP solution to be electrospun into a nanofibrous passive thermal control coating was prepared by dissolving the PVDF-HFP pellets in a solution of dimethyl formamide (DMF) and acetone (70/30 w/w) to form an 18% wt. solution. The solution was stirred at 40 °C and 400 rpm for 5 hours to form a viscous PVDF-HFP solution for electrospinning.

Solutions of SEBS were prepared by dissolving SEBS in xylene, a mixture of DMF and toluene, and a mixture of chloroform and toluene. Attempts were made to use these as adhesive layers between the electrospun PVDF-HFP nanofibers, or to electrospin these solutions as nanofibrous adhesives which would be used to bond the PVDF-HFP nanofibers to the aluminum foil substrate. The results will be discussed further in the subsequent sections.

2.2 Manufacturing and Characterization of PVDF-HFP Nanofibers

To manufacture the nanofibers, the following were used: a high-voltage power supply (set to 20 kV), a syringe pump with syringes and needles (1 ml/hr), and a rotating collector overlayed with aluminum foil and grounded. During electrospinning, the solution at the needle tip formed a Taylor cone from which the polymer jet ejected, forming nanofibers in flight towards the rotating collector under the influence of electrostatically-induced bending instabilities. These nanofibers were deposited on the aluminum foil substrate forming a thick, white membrane of PVDF-HFP nanofibers, as seen in Figure 1. At the end of the manufacturing process the nanofibrous membrane's properties were characterized.

The morphology of the nanofibrous PVDF-HFP was characterized using a Carl Zeiss Supra 55 Field Emission Scanning Electron Microscope (FESEM) and the micrographs were analyzed using Image J software to obtain the nanofiber distribution. Spectral hemispherical reflectance measurements were taken in the 300-2500 nm solar wavelength range using a Perkin-Elmer Lambda 950 UV-Visible-NIR spectrophotometer coupled with 6-inch thick Spectralon® integrating sphere accessory. The average solar reflectance (ρ_s) was calculated using the following equation:

$$\rho_s = \frac{\int_{\lambda_1=300\ nm}^{\lambda_2=2500\ nm} \rho_s(\lambda)\, I_s(\lambda) d\lambda}{\int_{\lambda_1=300\ nm}^{\lambda_2=2500\ nm} I_s(\lambda) d\lambda} \quad (1)$$

Where $I_s(\lambda)$ represents the solar spectral intensity at Air Mass 0 (AM 0) and $\rho_s(\lambda)$ represents the spectral hemispherical reflectance obtained from the spectrometer, relative to Spectralon's®. The mid infrared (2.5-15 μm) spectral reflectance and transmittance were characterized using a Fourier-Transform Infrared spectrometer (ThermoFisher Scientific Nicolet™ iS20) equipped with a 3-inch gold-coated integrating sphere (Pike Technologies Mid-IR IntegratIR™) and a mercury cadmium telluride (MCT) detector. The average emittance (ε_{IR}) of the nanofibers was calculated using:

$$\varepsilon_{IR} = \frac{\int_{\lambda_1=2.5\ \mu m}^{\lambda_2=15\ \mu m} (\varepsilon_{IR,\lambda})\, E_{b\lambda}(\lambda,T) d\lambda}{\int_{\lambda_1=2.5\ \mu m}^{\lambda_2=15\ \mu m} E_{b\lambda}(\lambda,T) d\lambda} \quad (2)$$

$$E_{b\lambda}(\lambda,T) = \frac{2hc^2}{\lambda^5 (e^{\frac{hc}{\lambda K_B T}} - 1)} \quad (3)$$

where $\varepsilon_{IR,\lambda}$ represents the spectral hemispherical emittance and $E_{b\lambda}(\lambda,T)$ is the Planck's spectral blackbody emissive radiance. h, c, λ, K_B, T represent Planck's constant, speed of light in vacuum, wavelength, Boltzmann's constant, and absolute temperature of the blackbody, respectively.

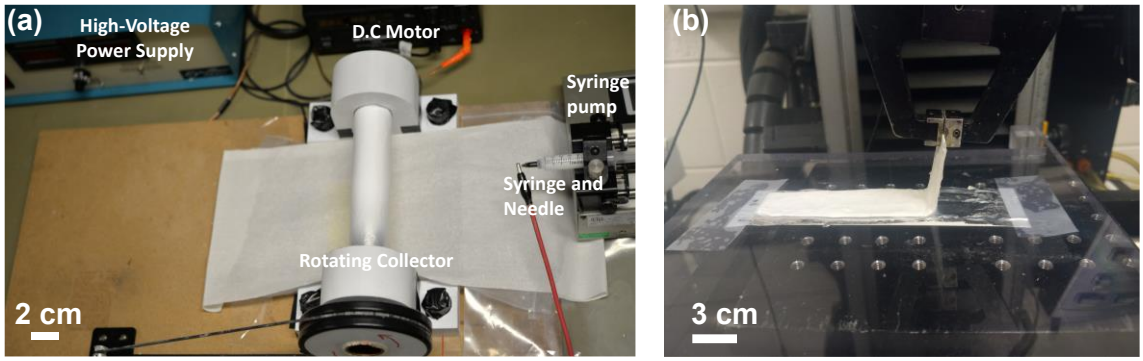

Figure 1. (a) Setup used for electrospinning PVDF-HFP, with nanofibers visible on the collector. (b) Ongoing peeling test.

2.3 Peeling Test Procedure

Peeling tests were conducted to evaluate the strength of the bonds between the adherends (nanofibrous membrane and aluminum foil substrate) supplemented by commercial adhesives, as well as in-lab fabricated adhesives. The tests were performed using an Instron® 5843 universal testing machine equipped with a 10 N load cell, following the ASTM D6862 standard, at normal room conditions. This testing method requires the flexible adherend (nanofibers in this case) to be situated at 90^0 to the rigid adherend (aluminum foil substrate). To prevent deflection of the aluminum substrate, it was fixtured to a rigid acrylic block using both double-sided tape (bottom of the foil) and scotch tape (edges), as seen in Figure 1b. The samples were tested using a crosshead speed of 1 mm/min and load-extension curves were recorded for each sample. The resistance-to-peel strength of each adhesive was calculated by dividing the average peel strength (in newtons) by the sample width.

2.4 Thermal Cycling and Vacuum Effects on Adhesives

Extraterrestrial environments expose materials to extreme temperature and vacuum conditions, and these could affect the performance of adhesives used to bond materials. To understand these effects, we conducted thermal cycling and vacuum experiments by exposing the samples which had different adhesives to these conditions.

Twenty thermal cycles were conducted by inserting the samples in a bath of liquid nitrogen (-196 ^{o}C), allowing them to cool rapidly (~16 ^{o}C/s) and attain cryogenic temperatures. After ~5 minutes, they were taken out of the liquid nitrogen bath and placed in a convection furnace set to 100 ^{o}C leading to temperature rise of ~0.6 ^{o}C/s. This simulates space conditions where materials experience rapid temperature swings when they move from direct exposure to solar radiation to being in a planet's shadow, as governed by the materials' radiative properties, temperatures and views of space. Additionally, samples with different adhesives were exposed to vacuum conditions (rough vacuum ~10 Pa, room temperature) to study the effects of vacuum on adhesive strength. Subsequently, the adhesive peeling strengths were characterized following the peeling test procedure already described.

3. Results and Discussion

3.1 Morphology, Structure and Optical Properties

The morphology and structure of the electrospun PVDF-HFP nanofibrous thermal control coating is shown in Figure 2a. The coating consists of a porous structure with smooth-textured, nanoscale fibers with fiber distribution as shown in Figure 2b. Incident solar radiation which interacts with the fibers is scattered strongly because of the refractive index mismatch between the fibers and the pores. Also, the PVDF-HFP nanofiber sizes, being comparable to the wavelength of incident light, contributes to the scattering phenomenon, hence the strong solar reflectance (Figure 2c).

The optical selectivity of the PVDF-HFP nanofibers is revealed in Figures 2c and 2d – they exhibit very high solar reflectance (>99%) at solar wavelengths and this reflectance drops as they approach the infrared band of the spectrum, indicating strong infrared emittance ($\varepsilon_{IR} = 86\%$) which is necessary for self-cooling. This combination of very high solar reflectance and emittance imparts remarkable thermal control capabilities on the PVDF-HFP nanofibers. Double-aluminized Mylar ($\rho_s = 89\%, \varepsilon_{IR} = 3\%$) and aluminum foil ($\rho_s = 90\%, \varepsilon_{IR} = 5\%$) with broadband optical properties are shown in both graphs for comparison.

3.2 Adhesion Study

The electrospun PVDF-HFP nanofibers despite having excellent optical and thermally insulating properties are prone to delamination because of the weak adhesive forces between the nanofibers and the smooth aluminum foil substrate. The highly fluorinated co-polymer exhibits significantly low

surface energy, reducing its wettability and making it hydrophobic. To improve their adhesion to the substrate, we applied various adhesives between the nanofibers and the substrate.

SEBS [11], a thermoplastic elastomer which leverages the desirable properties of plastic and rubber materials, was used in this study as an adhesive. The properties such as high abrasion and fatigue resistance, high temperature tolerance and elastic recovery over a wide temperature range, as well as its good chemical, UV and weathering resistance make it a viable material which finds many useful applications including in the manufacture of adhesive tapes, sealants and coatings.

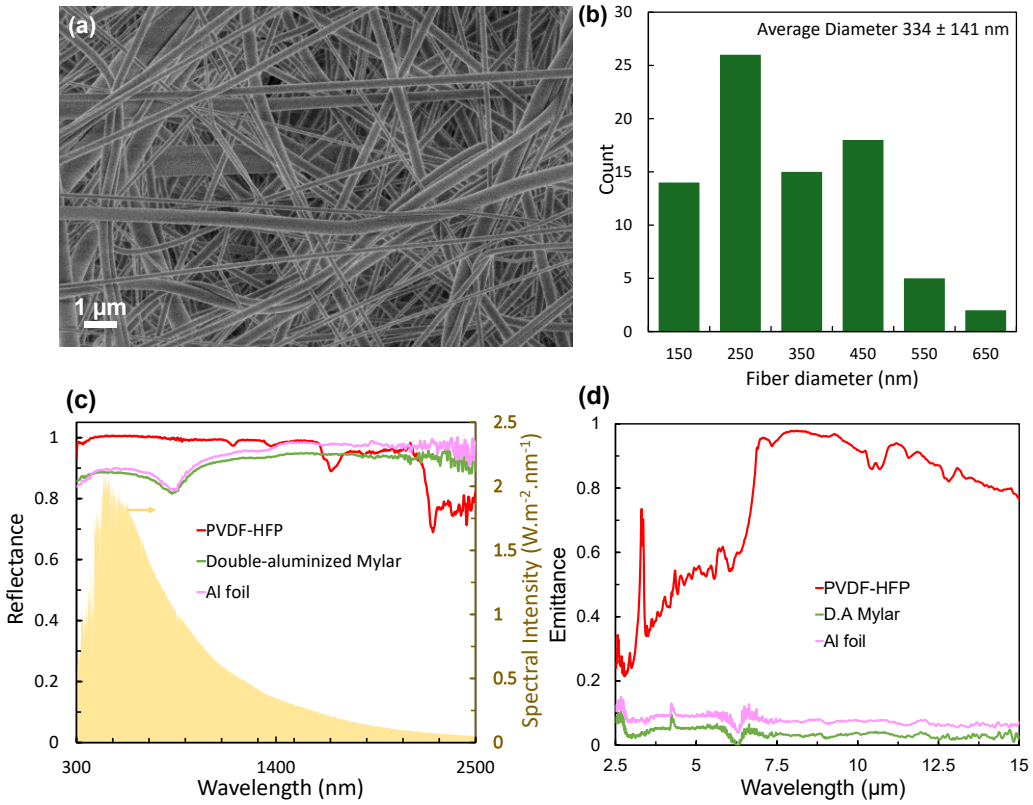

Figure 2. (a) SEM image showing the structure and nanofibers of electrospun PVDF-HFP. (b) Fiber diameter distribution. (c) Spectral reflectance of PVDF-HFP nanofibers and metallized reflectors (d) Infrared spectral emittance of the samples.

To use SEBS as an adhesive, we prepared a SEBS-xylene solution (25% w/w) and cast it on the substrate before placing the electrospun PVDF-HFP nanofibers on the SEBS-xylene adhesive and allowing both to cure and solidify. We faced problems using this approach because of the short pot life of the SEBS-xylene mixture, making it too viscous within a short time, leading to applicability problems. Also, this application method exposes the nanofibers to xylene which destroys the PVDF-HFP nanofibers causing them to shrink into a lump – this would affect the porosity of the nanofibers as well as it's optical properties, particularly its solar reflectance. Therefore, we did not continue with this method.

After this, we attempted to electrospin SEBS-xylene to form SEBS nanofibers on the Al foil substrate to which PVDF-HFP nanofiber mesh could be placed on and pressed together. This reasoning stems from the fact that having SEBS as a nanofibrous adhesive on the substrate would provide multiple nanoscale fiber-fiber contact points to which the PVDF-HFP nanofibers would attach and/or interweave, leading to the formation of many bridging zones, hence improving the adhesion of the PVDF-HFP nanofibers to the substrate. However, electrospinning SEBS-xylene was unsuccessful due to the high viscosity of the solution – the viscous forces within the solution overcame the electrostatic

forces needed to form a Taylor cone at the tip of the needle and eject SEBS nanofibers. This made it difficult to form SEBS-xylene nanofibers.

Next, we used DMF-toluene (3:7 v/v) as solvent to form SEBS-DMF/toluene (22% and 14% w/w) adhesive solutions and attempted to electrospin these solutions to form SEBS nanofibers. This was again unsuccessful – the 22% w/w solution was too viscous, resembling a gel rather than a liquid, hence hindering electrospinning while the 14% w/w formed droplets (electrospray) rather than SEBS nanofibers. Then we used chloroform-toluene (80/20% w/w) as solvent to form a 15% w/w SEBS-chloroform/toluene adhesive solution for electrospinning. We were able to achieve few microscale SEBS fibers on the substrate with this solution but the continual clogging of the needles by the SEBS solution limited the electrospinning process, leading to very low throughput of SEBS adhesive fibers. We also made SEBS-chloroform/toluene solutions of lower concentrations for electrospinning, but these solutions did not form fibers.

After these attempts at electrospinning the SEBS adhesive, we decided to apply the SEBS adhesive as a thin layer (~0.02 mm) on the surface of the aluminum foil substate by painting with a brush. To do this, we made a 5% w/w SEBS-chloroform/toluene adhesive solution and applied it on the substrate. This solution had mild viscosity compared to others with higher concentrations, making it easily applicable on the substrate. The viscosity of the solution increased with time as the SEBS started to cure. On this SEBS layer, we placed the electrospun PVDF-HFP nanofibrous coating and pressed it down allowing the adhesive layer to cure, harden and dry. Other commercial adhesives were also applied as thin layers (~0.02 – 0.04 mm) on aluminum foil substrates and the PVDF-HFP nanofibrous samples were placed on these layers and allowed to dry. After 2-3 days of drying, the samples were characterized using the Instron machine.

3.3 Peeling Test Results

Figure 3 shows the peeling test results obtained from the Instron machine. Figure 3a depicts a sample bonded with SEBS adhesive (after the peeling test) which was not exposed to extreme conditions. Typically, three types of failure are possible when studying adhesive bond strengths between adherends – adhesive failure, cohesive failure and substrate failure [12]. Adhesive failure occurs at the interface between the adhesive and substrate, an example of which would be either adherend peeling off from the adhesive. Cohesive failure occurs within the adhesive and could be because of degradation of the adhesive with time or under extreme environmental conditions. Substrate failure manifests as a rupture of either adherend because of very good adhesive strength; for example, an interlaminar debonding of the nanofibers from the adhesive-substrate interface.

In all the peeling tests conducted, adhesive failure mode was observed for all samples - they all peeled off smoothly from their aluminum substrates, without leaving residual adhesive fragments on their substrates. The adhesives must have permeated upwards through the porous fiber network and cured within the material and at the bottom face of the nanofibers. Under the applied forces, this led to delamination of the nanofiber-adhesive pair from the foil. Figure 3a shows the peeled-off nanofibers with cured adhesive at the interface producing a glossy finish.

Figure 3b compares the peel force vs extension results for pristine samples under normal conditions. The peel test result for commercial electrical tape was also included in the graph for comparison to give an idea of the magnitude of bond strengths being measured. Figure 3c compares the samples after exposure to thermal cycles and vacuum (electrical tape was excluded from this study). To reduce noise in the dataset, a simple moving average technique was used to smoothen the fluctuations. In Figure 3d, adhesive peel strength comparison is made for all samples.

By observing Figures 3b – 3d, it is obvious that the peel strengths of the pristine samples are lower than those of the environmentally-conditioned samples. From Figure 3d, under normal conditions (solid histograms), a higher peel strength was calculated for SEBS adhesive (0.047 N/mm) compared

to Loctite (0.038 N/mm) and Permatex (0.016 N/mm) adhesives. The electrical tape had a peel strength of 0.048 N/mm, implying that the pristine SEBS adhesive shows comparable adhesive strength with the adhesive used on electrical tapes. However, under vacuum and thermal cycling, the results were different. Post-vacuum peel strengths were as follows: 0.105 N/mm, 0.129 N/mm and 0.069 N/mm for SEBS, Loctite and Permatex, respectively, amounting to increases of 123%, 241% and 324%, respectively. Under vacuum, air trapped in the pores of the nanofibers would have been pulled out allowing more wetting of the nanofibers by the adhesive, hence improving interfacial adhesion. Furthermore, residual curing reactions may have occurred under vacuum leading to better cross-linking, the elimination of volatile by-products of cross-linking and improved bond strengths.

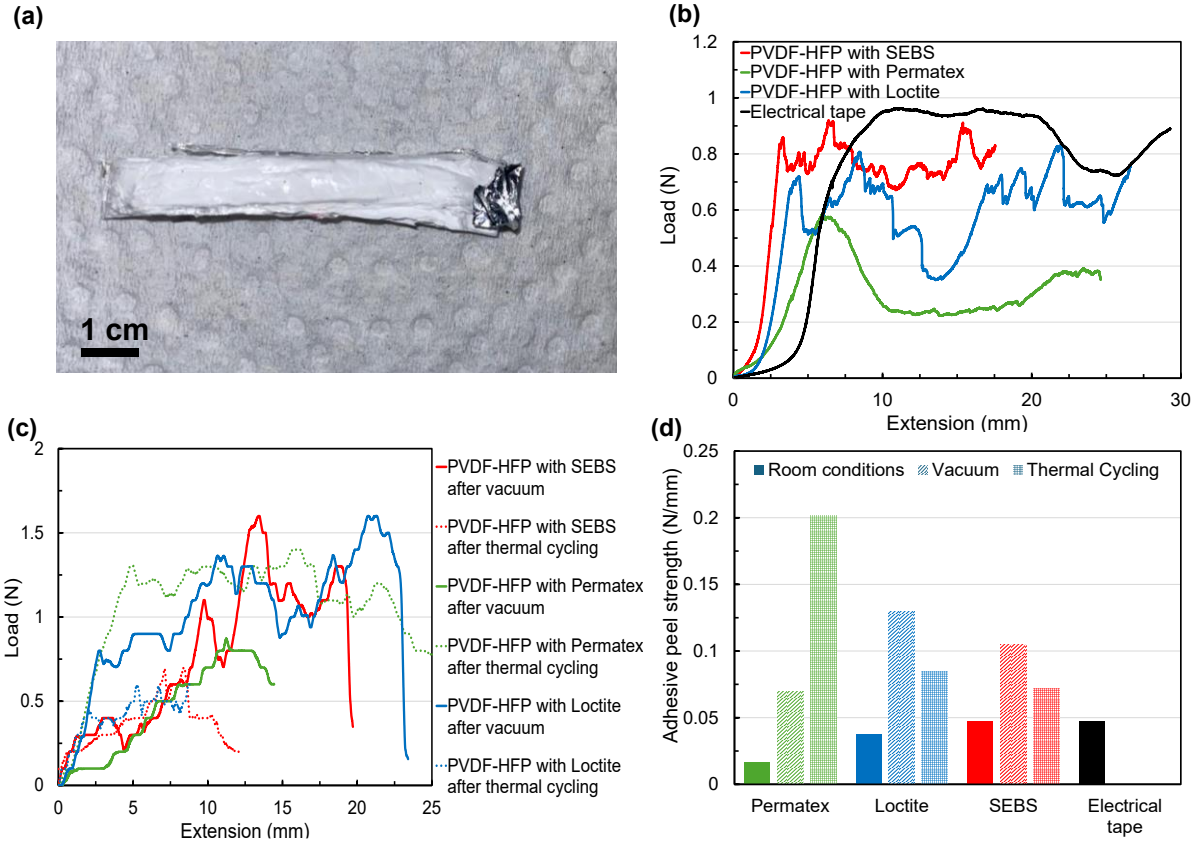

Figure 3. (a) Post-peeling test image of a PVDF-HFP nanofibrous sample bonded with SEBS adhesive. Load-extension curves for the peeling tests performed on samples with different adhesives at normal conditions (b) and post space-like conditions (c). (d) Adhesive peel strengths calculated from the load-extension curves.

Lastly, after thermal cycling, SEBS and Loctite peel strengths increased to 0.072 N/mm and 0.084 N/mm, respectively (52% and 122% increments, respectively) while that of Permatex increased significantly by an order of magnitude to 0.202 N/mm. These increments were contrary to expectations because it has been shown that thermal cycling could negatively impact the performance of adhesives [13,14]. It is possible that chemical reactions may have occurred, or new chemical bonds formed which contributed to the increased bond strength. The dwell times of the materials in extreme conditions may also have been too short to induce degradation in the adhesives. However, some silicones have been engineered to retain their properties in extreme thermal conditions. Permatex, a silicone-based room temperature vulcanized (RTV) elastomer, has been reported to be resistant to thermal cycling and this could be attributed to the increase in the adhesive strength of Permatex [15]. Further studies would provide more insight into this occurrence.

The increases recorded in peeling strengths for all samples after aging tests indicate that these environmental conditions may have induced some post-curing effects on the adhesives and nanofibers, which could have helped to strengthen the bonds. A deeper understanding would be provided by more extensive chemical, spectrometric, thermal and surface characterizations of the interfaces provided for adhesion to shed more light on the mechanisms of adhesion.

Conclusions

This study investigates the adhesion of nanofibrous PVDF-HFP thermal control coatings to aluminum substrates under normal and space-like environmental conditions. Commercial and in-lab fabricated adhesives were applied and peeling tests were conducted to assess the strengths of the interfacial bonds and understand the failure modes. The results show that the in-lab adhesive, SEBS, performs better under pristine conditions. However, exposing them to extraterrestrial conditions generally improves their peel strengths. Future research efforts would study the effects of longer extreme environment dwell times on the adhesive strengths, while conducting extensive characterizations to assess their performance and lifetime.

Acknowledgments

The authors acknowledge the support of the National Aeronautics and Space Administration under Grant No. 80NSSC21K0072 issued through the Space Technology Research Grants.

Declaration of Competing Interest

The authors declare the following financial interests/personal relationships which may be considered as potential competing interests: Rensselaer Polytechnic Institute has filed the following non-provisional patent application related to this work – Non-Provisional Application No: 19/178,759.

References

[1] Ibekwe C, Wang X, Bolzani BN, O'Brien C, Waataja CJ, Mahony CP, et al. ACS Appl Mater Interfaces 2024. https://doi.org/10.1021/acsami.4c02463.
[2] Ibekwe, C, Wang, X, Hartwig, JW, Feller, JR, Swanger, AM, & Narayan, S. " *Proceedings of the ASME 2024 International Mechanical Engineering Congress and Exposition*. *Volume 9: Heat Transfer and Thermal Engineering*. Portland, Oregon, USA. November 17–21, 2024.ASME. https://doi.org/10.1115/IMECE2024-144206
[3] Ibekwe, C, Wang, X, Hartwig, JW, Swanger, AM, & Narayan, S." *Proceedings of the ASME 2024 International Mechanical Engineering Congress and Exposition*. *Volume 9: Heat Transfer and Thermal Engineering*. Portland, Oregon, USA. November 17–21, 2024. ASME. https://doi.org/10.1115/IMECE2024-146008
[4] Wang X, Narayan S.. Renew Energy 2022;197:574–82. https://doi.org/10.1016/j.renene.2022.07.143.
[5] Parisi G, Wang X, Hwang Y, Narayan S.. Adv Sustain Syst 2024;8:2400237. https://doi.org/10.1002/ADSU.202400237.
[6] Parisi G, Szewczyk PK, Narayan S, Stachewicz U. ACS Appl Mater Interfaces 2023;15. https://doi.org/10.1021/acsami.3c07044.
[7] Parisi G, Szewczyk PK, Narayan S, Ura DP, Knapczyk-Korczak J, Stachewicz U. Small Science 2024;4. https://doi.org/10.1002/smsc.202400021.
[8] Hamdi M, Saleh MN, Poulis JA.. J Adhes Sci Technol 2020;34:1853–70. https://doi.org/10.1080/01694243.2020.1732750.
[9] Pereira JPO, Campilho RGSG, Nóvoa PJRO, Silva FJG, Gonçalves DC. vol. 37, Elsevier B.V.; 2021, p. 722–9. https://doi.org/10.1016/j.prostr.2022.02.002.
[10] Amini G, Gharehaghaji AA. Int J Adhes Adhes 2018;86:40–4. https://doi.org/10.1016/j.ijadhadh.2018.08.005.
[11] KRATON™ G1652 M Polymer, Pacific A. End Use Requirements. n.d.
[12] Petrie EM. 2013:225–74. https://doi.org/10.1533/9780857093967.2.225.
[13] Marchione F, Munafò P. Constr Build Mater 2021;299. https://doi.org/10.1016/j.conbuildmat.2021.124268.
[14] Wen X, Yuan X, , et al.. Energies 2017, Vol 10, Page 1054 2017;10:1054. https://doi.org/10.3390/EN10071054.
[15] Technical Data Sheet Permatex ® Clear RTV Silicone Adhesive Sealant. 2019